



Published in final edited form as:

Ann Thorac Surg. 2016 October ; 102(4): 1274–1281. doi:10.1016/j.athoracsur.2016.04.001.

Regional Disruptions in Endothelial Nitric Oxide Pathway Associated With Bicuspid Aortic Valve

Mary P. Kotlarczyk, PhD, Marie Billaud, PhD, Benjamin R. Green, MS, Jennifer C. Hill, MFS, Sruti Shiva, PhD, Eric E. Kelley, PhD, Julie A. Phillippi, PhD, and Thomas G. Gleason, MD

Departments of Cardiothoracic Surgery and Pharmacology and Chemical Biology, Vascular Medicine Institute, Departments of Anesthesiology, and Bioengineering, McGowan Institute for Regenerative Medicine, and Center for Vascular Remodeling and Regeneration, University of Pittsburgh, Pittsburgh, Pennsylvania

Abstract

Background.—Endothelial nitric oxide (NO) synthase (eNOS) has been implicated in the development of bicuspid aortic valve (BAV) and with differential expression in the ascending aorta of BAV patients. However, little is known about functional disruptions in the eNOS pathway and the effect on BAV-associated aortic dilatation. We tested the hypothesis that eNOS function is regionally diminished in ascending thoracic aortic aneurysms associated with BAV.

Methods.—Thoracic aortic aneurysms specimens were collected from patients with BAV (n [21) or tricuspid aortic valve (n [12). Tissue samples were harvested from three circumferential regions corresponding to locations above the right, left, and noncoronary sinuses. Adventitial-stripped specimens containing media and intima only were analyzed for NO synthase 3 gene expression and total eNOS protein. Indicators of eNOS activity (pSer1177-eNOS) and NO bioavailability (phosphorylation of vasodilator-stimulated phosphoprotein at Ser239) were also measured.

Results.—NO synthase 3 and eNOS protein were elevated in the right aortic region of BAV specimens compared with tricuspid aortic valve specimens. Activation of eNOS, as indicated by pSer1177-eNOS, was higher in BAV specimens across all regions. Despite increases in eNOS and pSer1177-eNOS, BAV specimens displayed no change in pSer239-vasodilator-stimulated phosphoprotein compared with tricuspid aortic valve specimens.

Conclusions.—BAV is associated with regional disruptions in the eNOS pathway, most markedly in the right aortic region. The discrepancy between increased eNOS activity and the absence of increased NO bioavailability in this region provides insight into physiologic mechanisms potentially underlying the asymmetric dilatation pattern observed in BAV.

Bicuspid aortic valve (BAV) is the most prevalent congenital malformation, occurring in 1% to 2% of the population [1]. The presence of BAV imparts a risk of dilatation of the proximal ascending thoracic aorta [2, 3], often occurring in an asymmetric pattern, with more marked dilatation along the greater curve just above the sinotubular junction [4–6].

Ascending thoracic aortic aneurysms (TAAs) in BAV patients share histologic hallmarks with degenerative TAAs in patients with a morphologically normal tricuspid aortic valve (TAV) and in those with Marfan syndrome and other genetically triggered aortopathies. Specifically, these TAAs demonstrate cystic medial degeneration characterized by noninflammatory loss of smooth muscle cells (SMCs), elastic fiber fragmentation, and accumulation of basophilic ground substance within the medial layer of the aortic wall [3, 7–9].

Although mutation of the fibrillin-1 gene contributes to TAA in Marfan syndrome, this is not the case in BAV, despite the histopathologic similarities. Furthermore, expression profiles of extracellular matrix markers differ between aneurysmal samples from TAV and BAV patients [10]. We previously demonstrated an attenuated response to oxidative stress in ascending aortic SMCs from BAV patients compared with cells from TAV patients [11]. Vascular wall remodeling also varied between BAV- and TAV-associated TAA [12]. These findings suggest different etiologies leading to the final common pathway of vessel wall degeneration.

Mechanisms underlying the increased risk of TAA with BAV are not completely understood. One hypothesis underlying BAV-associated aortopathy is a genetic defect in a key molecular pathway related to aortic wall homeostasis. Familial patterns of BAV exist [13]; however, no definitive genetic cause of BAV has been identified. Other studies provide support for altered hemodynamics as the driving force behind BAV-related aortic dilation. Hemodynamic investigations demonstrate turbulent blood flow patterns accompanying BAV [14–16] with a presumed effect on wall shear stress [17].

Yet, despite correction of the valvulopathy and associated abnormal hemodynamics by aortic valve replacement, BAV patients remain at increased risk for progressive dilatation of the proximal ascending aorta [18]. Several studies have demonstrated increased aortic dilation in BAV patients compared with TAV patients with similar degrees of valve disease [19] or even in the absence of clinical valvulopathy (ie, stenosis or regurgitation) [20]. These data support the notion of an inherent material property defect in the aortic wall or its biology that imparts development of TAA in BAV patients distinctly. Altered hemodynamics by the BAV morphology may initiate or exacerbate such underlying cell-mediated mechanisms that together lead to reduced structural integrity in the ascending aorta.

Evidence implicates endothelial nitric oxide (NO) synthase (eNOS), the enzyme that produces NO, as a potential contributor to BAV development. Lee and colleagues [21] observed the BAV morphology in 5 of 12 eNOS-knockout mice. Others have reported differential eNOS expression in BAV patients through histologic and biologic assessment [22–24]. However, no definitive pattern of eNOS expression has emerged. Little evidence exists regarding alterations in eNOS function and NO bioavailability in BAV patients.

We hypothesized that eNOS expression or function, or both, is regionally diminished in BAV-associated TAA, corresponding to asymmetric dilatation. We profiled eNOS expression and functional markers in aneurysmal tissue from patients with BAV or TAV. Because pathologic changes and aneurysm shape can vary regionally in the ascending aorta, we examined specimens from three distinct circumferential locations. We present evidence of

disrupted regional NO bioavailability in TAA from BAV patients, providing insight into mechanistic changes in the eNOS pathway associated with BAV aortopathy.

Patients and Methods

Specimen Acquisition

Aneurysmal aortic specimens were obtained prospectively from 33 patients presenting to the Center for Thoracic Aortic Disease at the University of Pittsburgh Medical Center for elective aortic valve or ascending aortic replacement, or both. Patients with known connective tissue disorders (Marfan syndrome, Ehlers-Danlos, or Loeys-Dietz) were excluded. Informed consent was obtained from all patients. Tissue was acquired in accordance with an Institutional Review Board–approved protocol. Table 1 describes patient demographics. BAV morphotypes were classified according to Sievers and Schmidtke [25] to facilitate comparisons with contemporary findings [16, 17].

Specimens were collected from three circumferential regions (R, L, and N) of the ascending aorta corresponding to the anatomic position of the right, left, and noncoronary sinuses. When no raphe existed in BAV samples, circumferential regions were defined based on the left coronary artery at 120-degree increments. All regions were collected from each patient with the exception of 1 BAV patient, in which only R and L regions were available.

Specimens were taken within 1 to 2 cm of the sinotubular junction to capture as many samples as possible. The adventitia was removed, and specimens containing only media and intima were stored at -20°C in RNAlater (Life Technologies, Carlsbad, CA) for gene expression analysis or were snap frozen and stored at -80°C for protein extraction.

Gene Expression Analysis

Specimens were homogenized (gentleMACS Dissociator; Miltenyi Biotec, San Diego, CA), and total RNA was extracted (RNeasy Mini Kit; Qiagen, Valencia, CA) and quantified (Qubit 2.0 fluorimeter; Life Technologies). For each reaction, 5 ng RNA was combined with TaqMan RNA-to- C_t one-step reverse-transcription polymerase chain reaction reagents (Life Technologies) and TaqMan gene expression assays containing gene-specific primers and probe (NO synthase 3 [NOS3; eNOS], Assay Hs00167166_m1 or platelet endothelial cell adhesion molecule-1 [CD31], Assay Hs00169777_m1; Life Technologies). After real-time reverse-transcription polymerase chain reaction (ABI 7900HT system; Applied Biosystems, Foster City, CA), relative NOS3 expression was determined using the 2^{-C_t} method (SDS 2.2 software; Applied Biosystems).

Protein Analysis

Tissue samples were homogenized in radioimmunoprecipitation assay buffer containing protease and phosphatase inhibitor cocktails (Pierce Biotechnology, Rockford, IL), incubated on ice for 20 to 30 minutes to complete lysis, and centrifuged at 20,000g at 4°C for 20 minutes. Protein was quantified by bicinchoninic acid assay (Pierce Biotechnology). Lysates were stored at -80°C before analysis.

Protein expression was assessed using standard immunoblotting procedures. Lysates containing 40 mg of protein in Laemmli sample buffer were boiled 5 minutes before resolution on 4% to 12% TGX gels (BioRad, Hercules, CA). Proteins were transferred to polyvinylidene fluoride membrane by wet transfer in icecold buffer Tris-Glycine Electrobloiting buffer (National Diagnostics, Atlanta, GA) with 10% methanol. Blots were blocked for 1 hour (5% milk or bovine serum albumin in Tris-buffered saline with 0.1% Tween-20), then probed with primary antibody overnight at 4°C.

Primary antibodies included CD31 (catalog #3528) and pSer239-vasodilator-stimulated phosphoprotein (VASP; #3114; Cell Signaling Technology, Danvers, MA); eNOS (#610296), pSer1177-eNOS (#612392), and VASP (#610447; BD Biosciences, San Jose, CA); and β -actin (#ab8227; Abcam, Cambridge, MA). Blots were washed with Trisbuffered saline with 0.1% Tween-20 and probed with secondary antibody goat anti-mouse horseradish peroxidase (#31432), goat anti-rabbit horseradish peroxidase (#34162; Pierce Biotechnology), and goat anti-mouse horseradish peroxidase (#sc-2005, Santa Cruz Biotechnology, Dallas, TX).

After washing, bands were visualized (SuperSignal West ECL, Pierce) on a ChemiDoc imager (BioRad) and quantified using Image Lab software (BioRad) with rolling disk background subtraction. When appropriate, blots were stripped in strong stripping buffer (EMD Millipore, Billerica, MA) and reprobed. Total eNOS and pSer1177-eNOS were normalized to CD31 to control for variation in intimal endothelial cell content among specimens. VASP and pSer239-VASP were normalized to β -actin.

Statistical Analysis

Comparisons between group demographics were assessed by the Fisher exact test or the Mann-Whitney test. Outcome variables between BAV and TAV groups were compared using the Mann-Whitney test. Regional variations (R vs N, R vs L, and N vs L) within each valve type were examined using the Wilcoxon matched-pair signed rank test to account for repeated measurements from the same patient. Correlations were determined using the Spearman rank coefficient (r_s). Analyses were completed with SPSS 22 software (IBM Corp, Armonk, NY). Values of $p < 0.05$ were considered significant.

Results

BAV aortic specimens from the R region displayed increased NOS3 expression compared with TAV specimens ($p = 0.011$, Fig 1). Examination of regional differences within each patient group uncovered elevated NOS3 in the R region compared with the L region in BAV patients ($p = 0.021$). Age and aortic diameter had no correlation to NOS3 expression. Within valve types, NOS3 did not differ between those with none to mild insufficiency or stenosis and those with moderate to severe valvulopathy.

BAV specimens also displayed elevated eNOS protein in the aortic R region compared with TAV ($p = 0.004$, Fig 2). No regional differences within each valve group were identified. R region specimens from BAV patients with moderate to severe stenosis displayed higher eNOS than specimens from patients with mild to no stenosis ($p = 0.045$). Similar assessment

in the TAV cohort could not be performed due to lack of aortic stenosis in this patient group. Levels of eNOS did not differ with the degree of aortic valve insufficiency. Age and diameter exhibited no correlation with eNOS protein in either group at any region.

We explored relative levels of active eNOS by quantifying eNOS phosphorylation at Ser1177. The increase in total eNOS observed in the R region of BAV specimens (Fig 2) was matched by a concomitant increase in pSer1177-eNOS ($p = 0.006$, Fig 3). The N and L regions also demonstrated elevated pSer1177-eNOS compared with the corresponding region in TAV ($p = 0.012$ and $p = 0.024$, respectively; Fig 3). Expression of pSer1177eNOS did not vary regionally in either group. Within the BAV R region, age correlated positively with pSer1177-eNOS ($r_s = 0.465$, $p = 0.034$). No other correlations were found between pSer1177-eNOS and age, diameter, or presence of aortic valvulopathy.

Despite elevated eNOS and pSer1177-eNOS in the R region, BAV specimens exhibited no change in pSer239VASP compared with TAV (Fig 4). Expression of pSer239-VASP was similar among all circumferential regions for both BAV- and TAV-derived aortic specimens. Total VASP protein levels did not differ between groups at any region (Fig 4). No correlations between pSer239VASP and age, maximum aortic diameter, or presence of valvulopathy were found in either group.

Comment

A connection between eNOS and BAV was previously proposed in the context of BAV morphology presenting in eNOS-knockout mice [21]. Few studies have examined eNOS and its functionality in the ascending aorta of BAV patients. Using samples from normal caliber and dilated aorta, Aicher and colleagues [22] reported reduced eNOS protein in the lateral ascending aorta of BAV patients compared with TAV and a negative correlation between aortic diameter and eNOS in BAV patients. Spatial analysis by Mohamed and colleagues [23] revealed higher eNOS protein in the concave region of the ascending aorta compared with the convex region within a BAV group, but unlike Aicher and colleagues [22], reported no differences in eNOS between BAV and TAV specimens from corresponding regions [23]. In contrast to findings of decreased eNOS in BAV, eNOS gene expression in specimens from the convexity of the aorta was higher in BAV than in TAV [24]. In our cohort, compared with samples from TAV patients, BAV specimens exhibited increased eNOS gene and protein expression in the R aortic region (the anterolateral segment), which constitutes much of the so-called greater curvature or convexity of the ascending aorta. (Although the lateralmost aspect of the noncoronary segment also constitutes a portion of the greater curvature, to allow for consistent sample processing and avoid sampling error, regions were defined by the easily identified commissural lines of demarcation.)

These conflicting data may reflect the heterogeneity of BAV-associated aortopathy with respect to extent of dilatation, aneurysm morphology, and histopathologic changes. In addition, unlike previous studies that used full-thickness aortic specimens, we investigated the intimal and medial layers of the aorta to remove additional sources of eNOS present in the vascularized adventitia. Focusing on eNOS primarily in the intimal layer allows for interpretation of intimal function and related NO production specifically.

Measurement of eNOS expression provides important information about changes in the aorta of BAV patients but may not completely describe eNOS functionality. We discovered elevated eNOS in BAV, accompanied by an elevation in activated eNOS. Importantly, despite elevated eNOS and pSer1177-eNOS, there was no corresponding increase in pSer239-VASP. VASP phosphorylation at Ser239 is an established downstream marker of NO bioavailability [26]. The lack of increased pSer239VASP in BAV specimens suggests dysfunction of the eNOS/NO pathway and region-specific disruptions in NO bioavailability in the setting of BAV.

Several mechanisms induce phosphorylation of eNOS at Ser1177, and most notable in the context of this study is shear stress. Hemodynamic modeling and fourdimensional flow (phase contrast) magnetic resonance imaging of BAV patients have demonstrated turbulent flow patterns suggesting increased wall shear stress in the greater curvature of the ascending aorta in BAV patients [15–17]. BAV patients tend toward asymmetric dilatation of the proximal ascending aorta, particularly with type 1 morphotypes [4–6, 15, 27–29], localized to the greater curvature, whereas TAAs in TAV patients tend toward a more uniform, symmetrical dilatation pattern. Furthermore, differential expression of extracellular matrix proteins important to vessel wall integrity was found in the greater curvature of aortic specimens from BAV patients [30, 31].

Our observations of altered eNOS expression with disrupted NO bioavailability in the R region of BAV patients provide a tenable link between hemodynamic and molecular explanations for the noted increased incidence of asymmetric aortic dilatation with BAV. Further study will be required to explore a direct mechanistic link between altered hemodynamics due to the BAV and effect on endothelial cell function and integrity of the neighboring medial layer of the aortic wall.

We previously demonstrated increased oxidative stress and altered response to free radicals by medial SMCs from the ascending aorta of BAV patients [11, 32]. Under conditions of oxidative stress, eNOS can become “uncoupled” from NO production and generate the free radical superoxide anion ($O_2^{\bullet-}$) [33]. Enzyme uncoupling can occur for several reasons, including arginine deficiency and depletion of the essential cofactor tetrahydrobiopterin [34]. Superoxide-mediated oxidation of tetrahydrobiopterin can result in its diminution. In addition, NO reacts at diffusion-limited rates with $O_2^{\bullet-}$ to form peroxynitrite ($O \frac{1}{4} NOO^-$), which can oxidize tetrahydrobiopterin leading to eNOS uncoupling [33, 34]. Once eNOS becomes uncoupled, enzymatic activity shifts, wherein NO production declines and $O_2^{\bullet-}$ is generated, fostering a condition of heightened oxidative stress.

We recently observed increased $O_2^{\bullet-}$ in ascending aortic specimens from BAV patients [35] with associated region-specific dysregulation of superoxide dismutases [36]. Collectively, we propose that eNOS in the R region of specimens from BAV patients is uncoupled from NO production and favors production of $O_2^{\bullet-}$ (Fig 5). Concordantly, as we attribute loss of oxidant defense in BAV SMCs, at least in part, to decreased basal and stress-induced expression of metallothionein [11, 32], downregulation of metallothionein, an antioxidant and target of NO [34], could also contribute to bioavailability of eNOS-produced NO. In

turn, decreased NO bioavailability could influence the role of metallothionein in intracellular zinc homeostasis [37, 38].

This study provides a deeper understanding of eNOS function in BAV-associated aneurysm, but there are limitations. The two populations observed varied in age, maximum diameter, and valve disease. Potential confounding variables from the BAV cohort include clinical indication for elective aortic replacement at a younger age [39, 40] and significant valve stenosis [2, 3]; therefore, the baseline differences between BAV and TAV patients are not unexpected. The influence of valvulopathy could not be assessed with the limited number of cases. Despite these potential confounders, aortic diameter did not correlate with any outcome measured. Age was correlated only with pSer1177-eNOS in BAV R region specimens. Aortic stenosis correlated with eNOS protein in R region specimens from BAV patients but not with other outcomes.

We have demonstrated regional alterations in the eNOS-mediated NO signaling cascade in the aortic wall of TAAs from BAV patients. The lack of elevated pSer239VASP infers disruption in NO bioavailability, perhaps due to decreased NO production by uncoupled eNOS or through diversion of NO to other reactions, such as with $O_2^{\bullet-}$. These data support our overarching hypothesis that BAV-associated aortopathy is mediated by altered response to reactive oxygen species and a heightened state of oxidative stress in the aortic wall by identifying eNOS as a potential source of $O_2^{\bullet-}$ production.

Acknowledgments

This work was supported by the National Heart, Lung, and Blood Institute of the National Institutes of Health under Award HL-109132 (T.G.G.) and the American Heart Association Award 13POST14570000 (M.P.K.). The authors thank Dr Forozan Navid (Department of Cardiothoracic Surgery, University of Pittsburgh Medical Center) for help with specimen acquisition, Dr Andrew Althouse for assistance with statistical analyses, and Kristin Valchar and Julie Schreiber for assistance with Institutional Review Board protocols and informed consent. The real-time reverse-transcription polymerase chain reaction was performed in the Genomics Research Core at the University of Pittsburgh.

References

1. Roberts WC. The congenitally bicuspid aortic valve. A study of 85 autopsy cases. *Am J Cardiol* 1970;26:72–83. [PubMed: 5427836]
2. Ward C Clinical significance of the bicuspid aortic valve. *Heart* 2000;83:81–5. [PubMed: 10618341]
3. Fedak PW, Verma S, David TE, Leask RL, Weisel RD, Butany J. Clinical and pathophysiological implications of a bicuspid aortic valve. *Circulation* 2002;106:900–4. [PubMed: 12186790]
4. Bauer M, Glied V, Siniawski H, Hetzer R. Configuration of the ascending aorta in patients with bicuspid and tricuspid aortic valve disease undergoing aortic valve replacement with or without reduction aortoplasty. *J Heart Valve Dis* 2006;15:594–600. [PubMed: 17044362]
5. Cotrufo M, Della Corte A. The association of bicuspid aortic valve disease with asymmetric dilatation of the tubular ascending aorta: identification of a definite syndrome. *J Cardiovasc Med* 2009;10:291–7.
6. Lu MT, Thadani SR, Hope MD. Quantitative assessment of asymmetric aortic dilation with valve-related aortic disease. *Acad Radiol* 2013;20:10–5. [PubMed: 22951111]
7. Bonderman D, Gharehbaghi-Schnell E, Wollenek G, Maurer G, Baumgartner H, Lang IM. Mechanisms underlying aortic dilatation in congenital aortic valve malformation. *Circulation* 1999;99:2138–43. [PubMed: 10217654]

8. Nataatmadja M, West M, West J, et al. Abnormal extracellular matrix protein transport associated with increased apoptosis of vascular smooth muscle cells in Marfan syndrome and bicuspid aortic valve thoracic aortic aneurysm. *Circulation* 2003;108(Suppl 1):II329–34. [PubMed: 12970255]
9. Blunder S, Messner B, Aschacher T, et al. Characteristics of TAV- and BAV-associated thoracic aortic aneurysms—smooth muscle cell biology, expression profiling, and histological analyses. *Atherosclerosis* 2012;220:355–61. [PubMed: 22178424]
10. Ikonomidis JS, Jones JA, Barbour JR, et al. Expression of matrix metalloproteinases and endogenous inhibitors within ascending aortic aneurysms of patients with bicuspid or tricuspid aortic valves. *J Thorac Cardiovasc Surg* 2007;133: 1028–36. [PubMed: 17382648]
11. Phillippi JA, Eskay MA, Kubala AA, Pitt BR, Gleason TG. Altered oxidative stress responses and increased type I collagen expression in bicuspid aortic valve patients. *Ann Thorac Surg* 2010;90:1893–8. [PubMed: 21095332]
12. Phillippi JA, Green BR, Eskay MA, et al. Mechanism of aortic medial matrix remodeling is distinct in patients with bicuspid aortic valve. *J Thorac Cardiovasc Surg* 2014;147: 1056–64. [PubMed: 23764410]
13. Cripe L, Andelfinger G, Martin LJ, Shooner K, Benson DW. Bicuspid aortic valve is heritable. *J Am Coll Cardiol* 2004;44: 138–43. [PubMed: 15234422]
14. Hope MD, Hope TA, Meadows AK, et al. Bicuspid aortic valve: four-dimensional MR evaluation of ascending aortic systolic flow patterns. *Radiology* 2010;255:53–61. [PubMed: 20308444]
15. Barker AJ, Markl M, Burk J, et al. Bicuspid aortic valve is associated with altered wall shear stress in the ascending aorta. *Circ Cardiovasc Imaging* 2012;5:457–66. [PubMed: 22730420]
16. Bissell MM, Hess AT, Biasioli L, et al. Aortic dilation in bicuspid aortic valve disease: flow pattern is a major contributor and differs with valve fusion type. *Circ Cardiovasc Imaging* 2013;6:499–507. [PubMed: 23771987]
17. Pasta S, Rinaudo A, Luca A, et al. Difference in hemodynamic and wall stress of ascending thoracic aortic aneurysms with bicuspid and tricuspid aortic valve. *J Biomech* 2013;46: 1729–38. [PubMed: 23664314]
18. Yasuda H, Nakatani S, Stugaard M, et al. Failure to prevent progressive dilation of ascending aorta by aortic valve replacement in patients with bicuspid aortic valve: comparison with tricuspid aortic valve. *Circulation* 2003;108 Suppl 1: II291–4. [PubMed: 12970248]
19. Keane MG, Wieggers SE, Plappert T, Pochettino A, Bavaria JE, Sutton MG. Bicuspid aortic valves are associated with aortic dilatation out of proportion to coexistent valvular lesions. *Circulation* 2000;102:III35–9. [PubMed: 11082359]
20. Nistri S, Sorbo MD, Marin M, Palisi M, Scognamiglio R, Thiene G. Aortic root dilatation in young men with normally functioning bicuspid aortic valves. *Heart* 1999;82:19–22. [PubMed: 10377302]
21. Lee TC, Zhao YD, Courtman DW, Stewart DJ. Abnormal aortic valve development in mice lacking endothelial nitric oxide synthase. *Circulation* 2000;101:2345–8. [PubMed: 10821808]
22. Aicher D, Urbich C, Zeiher A, Dimmeler S, Schäfers HJ. Endothelial nitric oxide synthase in bicuspid aortic valve disease. *Ann Thorac Surg* 2007;83:1290–4. [PubMed: 17383329]
23. Mohamed SA, Radtke A, Saraei R, et al. Locally different endothelial nitric oxide synthase protein levels in ascending aortic aneurysms of bicuspid and tricuspid aortic valve. *Cardiol Res Pract* 2012;2012:165957. [PubMed: 22745920]
24. Henn D, Perttunen H, Gauer S, et al. GATA5 and endothelial nitric oxide synthase expression in the ascending aorta is related to aortic size and valve morphology. *Ann Thorac Surg* 2014;97:2019–25. [PubMed: 24766859]
25. Sievers HH, Schmidtke C. A classification system for the bicuspid aortic valve from 304 surgical specimens. *J Thorac Cardiovasc Surg* 2007;133:1226–33. [PubMed: 17467434]
26. Oelze M, Mollnau H, Hoffmann N, et al. Vasodilatorstimulated phosphoprotein serine 239 phosphorylation as a sensitive monitor of defective nitric oxide/cGMP signaling and endothelial dysfunction. *Circ Res* 2000;87:999–1005. [PubMed: 11090544]
27. Della Corte A, Bancone C, Buonocore M, et al. Pattern of ascending aortic dimensions predicts the growth rate of the aorta in patients with bicuspid aortic valve. *JACC Cardiovasc Imaging* 2013;6:1301–10. [PubMed: 24269260]

28. Mahadevia R, Barker AJ, Schnell S, et al. Bicuspid aortic cusp fusion morphology alters aortic three-dimensional outflow patterns, wall shear stress, and expression of aortopathy. *Circulation* 2014;129:673–82. [PubMed: 24345403]
29. Stephens EH, Hope TA, Kari FA, et al. Greater asymmetric wall shear stress in Sievers' type 1/LR compared with 0/LAT bicuspid aortic valves after valve-sparing aortic root replacement. *J Thorac Cardiovasc Surg* 2015;150:59–68. [PubMed: 25956338]
30. Cotrufo M, Della Corte A, De Santo LS, et al. Different patterns of extracellular matrix protein expression in the convexity and the concavity of the dilated aorta with bicuspid aortic valve: preliminary results. *J Thorac Cardiovasc Surg* 2005;130:504–11. [PubMed: 16077420]
31. Della Corte A, Quarto C, Bancone C, et al. Spatiotemporal patterns of smooth muscle cell changes in ascending aortic dilatation with bicuspid and tricuspid aortic valve stenosis: focus on cell-matrix signaling. *J Thorac Cardiovasc Surg* 2008;135:8–18. [PubMed: 18179910]
32. Phillippi JA, Klyachko EA, Kenny JPt, Eskay MA, Gorman RC, Gleason TG. Basal and oxidative stress-induced expression of metallothionein is decreased in ascending aortic aneurysms of bicuspid aortic valve patients. *Circulation* 2009;119:2498–506. [PubMed: 19398671]
33. Cai H, Harrison DG. Endothelial dysfunction in cardiovascular diseases: the role of oxidant stress. *Circ Res* 2000;87: 840–4. [PubMed: 11073878]
34. Forstermann U, Li H. Therapeutic effect of enhancing endothelial nitric oxide synthase (eNOS) expression and preventing eNOS uncoupling. *Br J Pharmacol* 2011;164: 213–23. [PubMed: 21198553]
35. Phillippi J, Kotlarczyk MP, Green BR, et al. Bicuspid aortic valve patients exhibit superoxide accumulation in the ascending aorta. *Cardiovasc Pathol* 2014;23:e1–29.
36. Phillippi JA, Hill JC, Billaud M, Green BR, Kotlarczyk MP, Gleason TG. Bicuspid aortic valve morphotype correlates with regional antioxidant gene expression profiles. Presented at: the 41st Annual Meeting of the Western Thoracic Surgical Association, Whistler, British Columbia, Canada; June 24–27, 2015.
37. Pearce LL, Wasserloos K, St Croix CM, Gandley R, Levitan ES, Pitt BR. Metallothionein, nitric oxide and zinc homeostasis in vascular endothelial cells. *J Nutr* 2000; 130(5 Suppl):1467S–70S. [PubMed: 10801961]
38. St Croix CM, Wasserloos KJ, Dineley KE, Reynolds IJ, Levitan ES, Pitt BR. Nitric oxide-induced changes in intracellular zinc homeostasis are mediated by metallothionein/ thionein. *Am J Physiol Lung Cell Mol Physiol* 2002;282: L185–92. [PubMed: 11792622]
39. Svensson LG, Adams DH, Bonow RO, et al. Aortic valve and ascending aorta guidelines for management and quality measures: executive summary. *Ann Thorac Surg* 2013;95: 1491–505. [PubMed: 23291103]
40. Nishimura RA, Otto CM, Bonow RO, et al. 2014 AHA/ACC Guideline for the management of patients with valvular heart disease: executive summary: a report of the American College of Cardiology/American Heart Association Task Force on Practice Guidelines. *Circulation* 2014;129: 2440–92. [PubMed: 24589852]

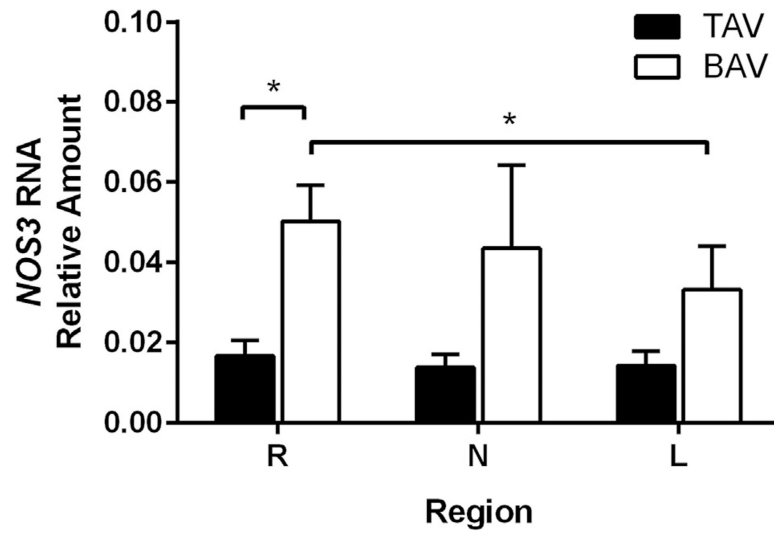


Fig 1. Nitric oxide synthase 3 (NOS3) gene expression (n ¼ 10–11 per valve type, per right [R], left [L], and noncoronary (N) sinus regions). Values are normalized to platelet endothelial cell adhesion molecule-1 expression. The error bars indicate SD. *p < 0.05 (BAV = bicuspid aortic valve; TAV = tricuspid aortic valve.)

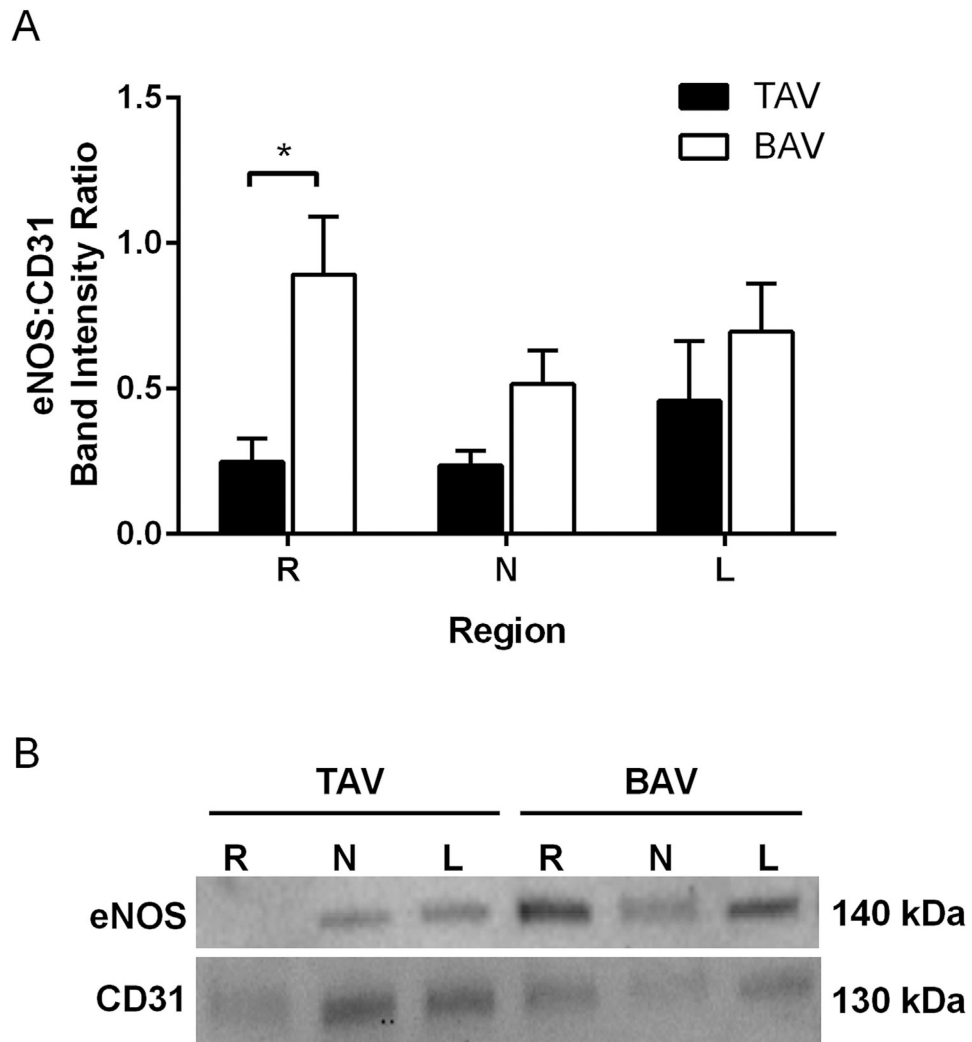


Fig 2. Expression of endothelial nitric oxide synthase (eNOS). (A) Analysis of eNOS immunoblots normalized to CD31; n = 12 tricuspid aortic valve (TAV) specimens or n = 20 to 21 bicuspid aortic valve (BAV) specimens per right (R), left (L), and noncoronary (N) sinus regions. *p < 0.05. The error bars indicate SD. (B) Representative immunoblots.

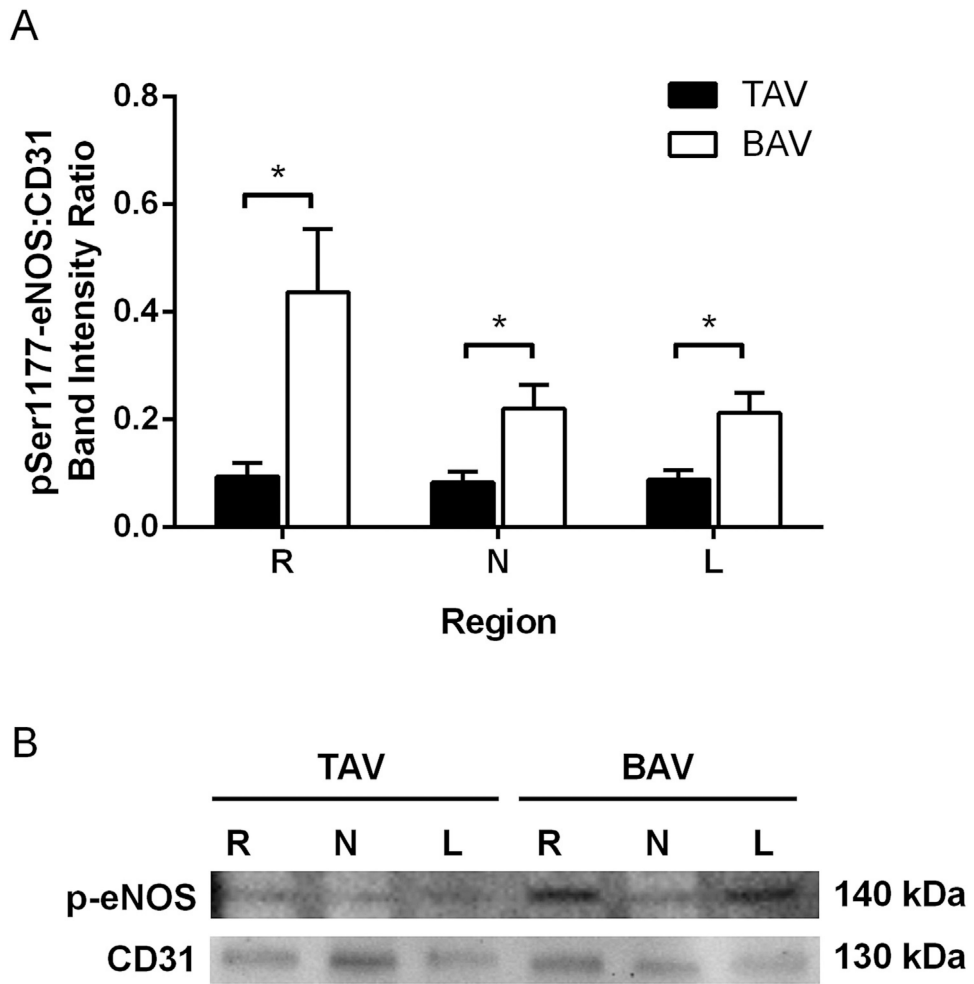


Fig 3. Phosphorylated (p) Ser1177-endothelial nitric oxide synthase (eNOS) quantification. (A) Analysis of pSer1177-eNOS immunoblots normalized to CD31; n = 12 tricuspid aortic valve (TAV) specimens or 20 to 21 bicuspid aortic valve (BAV) specimens per right (R), left (L), and noncoronary (N) sinus regions. *p < 0.05 (B) Representative immunoblots.

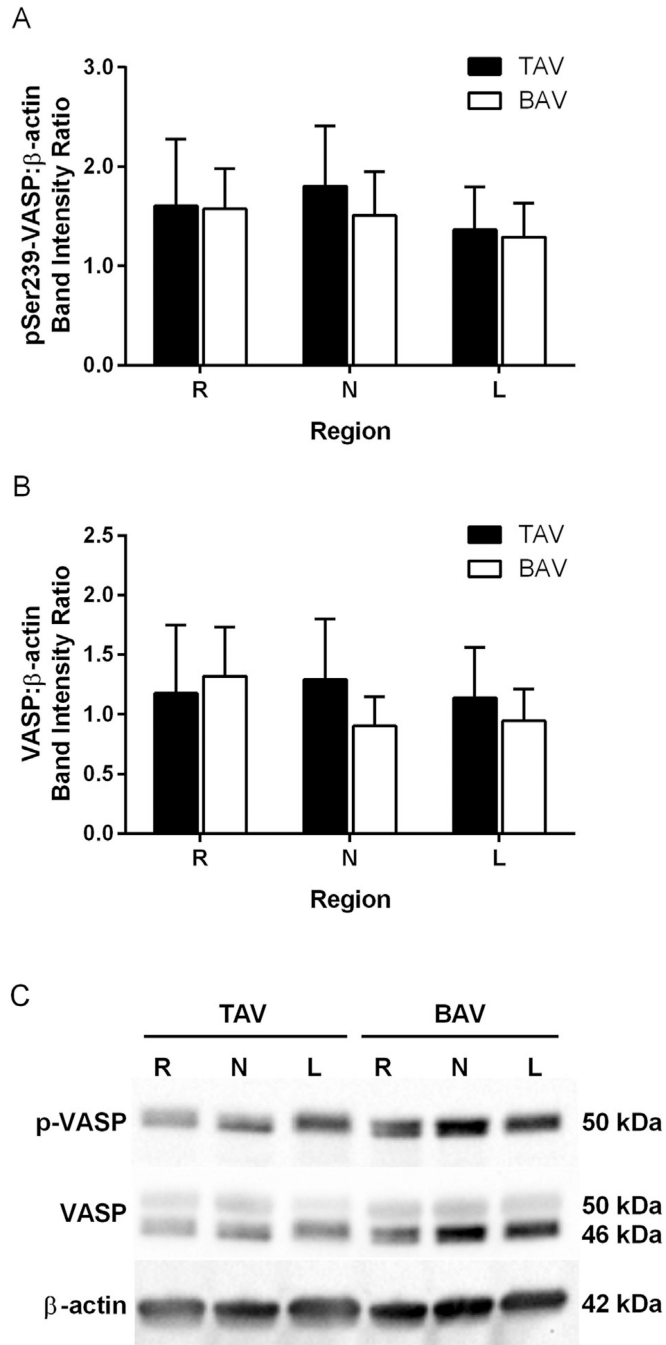


Fig 4. pSer239 vasodilator-stimulated phosphoprotein (VASP) as an indicator of nitric oxide bioavailability. Analysis of (A) pSer239-VASP and (B) VASP immunoblots normalized to β -actin; $n = 12$ tricuspid aortic valve (TAV) specimens or 20 to 21 bicuspid aortic valve (BAV) specimens per right (R), left (L), and noncoronary (N) sinus regions. (C) Representative immunoblots. (p = phosphorylated.)

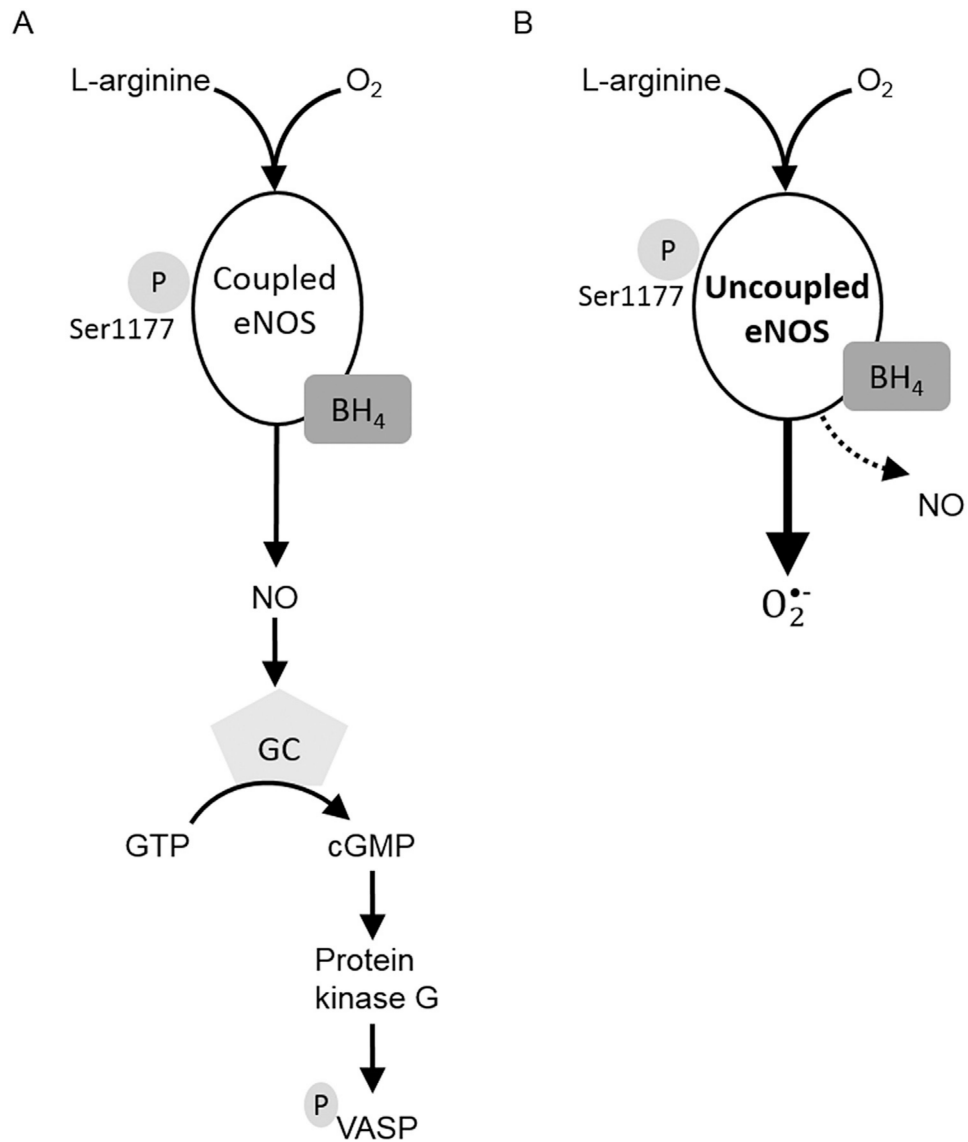


Fig 5. Proposed disruption of endothelial nitric oxide (NO) synthase (eNOS) pathway in bicuspid aortic valve (BAV) aortopathy. (A) Typically, eNOS produces NO in endothelial cells. NO increases activation of guanylyl cyclase (GC) in smooth muscle cells, leading to phosphorylation of vasodilator-stimulated phosphoprotein (VASP). (B) Under pathologic conditions such as bicuspid aortic valve, eNOS function may become uncoupled from NO synthesis. Production of superoxide anion predominates and NO levels decline. Uncoupled eNOS function can lead to oxidative stress and altered vascular wall remodeling. (BH_4 = tetrahydrobiopterin; cGMP = cyclic guanosine monophosphate; GTP = guanosine 5'-triphosphate.)

Table 1.

Patient Demographics

Variable	TAV (n = 12)	BAV (n = 21)	p Value
Sex, No.			1.000
Male	8	13	
Female	4	8	
Age, mean (SE), y	66.8 (3.2)	55.2 (2.1)	0.002
Max aortic diameter, mean (SE), mm	54.6 (1.7)	47.2 (0.7)	0.001
Hypertension, % (n/N)	83.3 (10/12)	66.7 (14/21)	0.429
Statin use, % (n/N)	50.0 (6/12)	42.9 (9/21)	0.731
Smoking history, % (n/N)	72.7 (8/11)	50.0 (8/16)	0.427
Aortic insufficiency, % (n/N)			0.149
None, mild	50.0 (6/12)	76.2 (16/21)	
Moderate, severe	50.0 (6/12)	23.8 (5/21)	
Aortic stenosis, % (n/N)			0.001
None, mild	100.0 (12/12)	38.1 (8/21)	
Moderate, severe	0.0 (0/12)	61.9 (13/21)	
BAV morphotype, No.			
Type 0	...	3	
Type 1, L/R	...	13	
Type 1, R/N	...	4	
Type 1, L/N	...	1	

BAV = bicuspid aortic valve; L = left; N = noncoronary; R = right; TAV = tricuspid aortic valve.